

Regular and quasi black hole solutions for spherically symmetric charged dust distributions in Einstein–Maxwell theory

Dubravko Horvat,* Saša Ilijic,† and Zoran Narančić

*Department of Physics, Faculty of Electrical Engineering and Computing,
University of Zagreb, Unska 3, HR-10 000 Zagreb, Croatia*

(Dated: December 2, 2024)

Abstract

Spherically symmetric distributions of electrically counterpoised dust (ECD) are used to construct solutions to Einstein–Maxwell equations in Majumdar–Papapetrou formalism. Unexpected bifurcating behavior of regular and singular solutions with regard to source strength is found for localized, as well as for the delta-function ECD distributions. Unified treatment of general ECD distributions is accomplished and it is shown that for certain source strengths one class of regular solutions approaches Minkowski spacetime, while the other comes arbitrarily close to black hole solutions.

PACS numbers: 04.40.Nr

*Electronic address: dubravko.horvat@fer.hr

†Electronic address: sasa.ilijic@fer.hr

I. INTRODUCTION

Static bodies resulting from combined gravitational attraction and electrical (electrostatic) repulsion [1, 2, 3] correspond to the middle stage of a collapsing star. According to the Oppenheimer-Snyder scenario [4], a static spherically symmetric perfect fluid ball, with energy momentum tensor

$$T_{\mu\nu} = (\rho + p) u_\mu u_\nu + p g_{\mu\nu} \quad (1.1)$$

where ρ , p , u^μ and $g_{\mu\nu}$ are mass density, pressure, four-velocity and metric (in geometrized units: $G = 1 = c$), after stationary phase and at the end of nuclear burning, starts to collapse. The pressure breaks down ($p = 0$) and remaining $T_{\mu\nu}$ assumes a form characteristic for a (spherical) dust ball, contemplating its equilibrium state. Eventually the ball begins to shrink so one can expect formation of a black hole. The Majumdar–Papapetrou formalism [5, 6, 7] can be applied to study the properties of spacetimes generated by static distributions of electrically counterpoised dust (or extremal charged dust, ECD), i.e., pressureless matter in equilibrium under its own gravitational attraction and electrical repulsion [1, 2, 3]. Special attention has been paid to ECD distributions leading to spacetimes that are everywhere regular, but with exterior arbitrarily close to that of an extremal Reissner–Nordstrøm (ERN) black hole [8, 9].

In this paper we will consider the coupled Einstein–Maxwell field equations in the Majumdar–Papapetrou approach. The energy-momentum tensor is given by (1.1), with $p = 0$, and remaining ρ represents the ECD distribution. Our study will concentrate on diverse (analytic) spherically symmetric forms of ECD distributions and corresponding solutions will be found. The theoretical framework is presented in Sec. II. In Secs. III and IV we present the solutions to Einstein–Maxwell equations for diverse ECD distributions and we discuss the bifurcating behavior of the solutions with respect to source strength. In Sec. V we show that with adjusting of the source strength and appropriate rescaling of the solutions the spacetimes with exteriors arbitrarily close to the ERN case can be obtained. Conclusions are given in Sec. VI, and extension of the present work is proposed.

II. THEORETICAL FRAMEWORK

One usually starts by defining a spherically symmetric spacetime line element of the form

$$ds^2 = -B(r) dt^2 + A(r) dr^2 + r^2 d\omega^2 \quad (2.1)$$

where $d\omega^2 = d\vartheta^2 + \sin^2 \vartheta d\varphi^2$. For an asymptotically flat spacetime one requires

$$A(r)|_{r \rightarrow \infty} = B(r)|_{r \rightarrow \infty} = 1, \quad (2.2)$$

and for a nonsingular spacetime $A(r = 0) = 1$. A. Papapetrou has shown [6, 7] that in certain coordinates the line element can be written as

$$ds^2 = -e^\chi dt^2 + e^\varphi (dX^2 + dY^2 + dZ^2) \quad (2.3)$$

and that it is possible to connect functions χ and φ in such a way as to satisfy (as one possibility) $d\chi/d\varphi = -1$ or $\chi(\varphi) = -\varphi$. Together with Majumdar's assumption [5] about connection between g_{tt} (or g_{00}) metric component and a scalar component of the electromagnetic potential A^μ comprising the electromagnetic energy-momentum tensor $T_{\mu\nu}^{(\text{em})}$, the line element ds^2 in the Majumdar–Papapetrou form can be written in the harmonic coordinates (t, \mathbf{X}) as

$$ds^2 = -e^{-\varphi} dt^2 + e^\varphi (dX^2 + dY^2 + dZ^2) \quad (2.4)$$

(in the original notation of [7]). This line element shares no common symmetry with the line element given in (2.1), although we will assume the spherical symmetry as a general symmetry requirement for our problem. The essential ingredient to the line element (2.4), as shown by Majumdar, are additional assumptions which should be made about a specific form for the energy-momentum tensor $T_{\mu\nu}$ that enters the Einstein equations

$$R_{\mu\nu} - \frac{1}{2}g_{\mu\nu}R = 8\pi T_{\mu\nu} \quad (2.5)$$

(in geometrized units). The component of $T^{\mu\nu}$ due to electromagnetic fields is given by:

$$T_{\mu\nu}^{(\text{em})} = \frac{1}{4} g_{\mu\nu} F^{\rho\sigma} F_{\rho\sigma} - F_\mu^\sigma F_{\nu\sigma}, \quad (2.6)$$

where $F_{\mu\nu} = A_{\nu,\mu} - A_{\mu,\nu}$ is the antisymmetric electromagnetic field tensor, and a comma denotes an (usual) derivative, to differ from semicolon denoting a covariant derivative. It satisfies the empty space equation $F^{\mu\nu}_{;\nu} = 0$.

A more general situation differing from the one described above corresponds to

$$T_{\mu\nu} = T_{\mu\nu}^{(\text{em})} + T_{\mu\nu}^{(\text{m})} \quad (2.7)$$

where the superscript (m) denotes matter. The absence of $T_{\mu\nu}^{(\text{m})}$ leads to Reissner–Nordstrøm solutions with $B(r) = A(r)^{-1} = (1 - 2m/r + q^2/r^2)$ for $A^0 = e/r$. It is shown in Ref. [10] that for charged sphere of radius a , for r large enough, m could be set equal to zero, whereas for the interior solution, i.e. $r < a$, one is not permitted to put $m = 0$. It follows that electric charge contributes to the gravitational mass of the system. In addition to that, mass as given in $B(r) = A(r)^{-1}$ above satisfies a positivity condition $m > 0$. Citing Ref. [10] “a charged sphere must have a positive mass”.

In the case of the complete $T^{\mu\nu}$ given in (2.7) one assumes a perfect fluid of classical hydrodynamics representing (charged) dust (matter) for which in general energy-momentum tensor is given by (1.1). At the time when p ceases to exist, as explained in introduction (Oppenheimer–Snyder collapse), the energy momentum tensor (1.1) reduces to $T_{\mu\nu}^{(\text{m})} = \rho u_\mu u_\nu$, where ρ is now an invariant fluid density and u_μ is a four-velocity which will be assumed to be in non-moving (co-moving) coordinate system so that

$$u^\mu = c \frac{dX^\mu}{ds} \longrightarrow u^\mu = \delta_0^\mu u . \quad (2.8)$$

The electromagnetic part of $T_{\mu\nu}$ is given, as before, with (2.6). The four-current density of the the charge/matter/dust distribution is given by

$$J^\mu = \rho_e u^\mu . \quad (2.9)$$

At this point the crucial assumption is made by setting the electric charge density ρ_e equal to the matter density ρ , or somewhat more general $\rho_e = \pm \rho$. Now the metric (2.4) can be written in the form

$$ds^2 = -U^{-2} dt^2 + U^2 (dX^2 + dY^2 + dZ^2) . \quad (2.10)$$

The Einstein field equations incorporating the above introduced ingredients are given by

$$\begin{aligned} G_{\mu\nu} &= 8\pi (T_{\mu\nu}^{(\text{em})} + T_{\mu\nu}^{(\text{m})}) \\ &= 8\pi \left[\frac{1}{4\pi} \left(F_{\mu\alpha} F_\nu^\alpha - \frac{1}{4} g_{\mu\nu} F^{\alpha\beta} F_{\alpha\beta} \right) + \rho_e u_\mu u_\nu \right] , \end{aligned} \quad (2.11)$$

and by using the Majumdar (or Majumdar–Papapetrou) assertion, the generalized (nonlinear) Poisson equation (with $\rho = \rho_e$)

$$F^{\mu\nu}_{,\nu} = 4\pi J^\mu = 4\pi \rho u^\mu \quad (2.12)$$

assumes a simple form

$$\nabla^2 U = -4\pi \rho U^3. \quad (2.13)$$

Here U and ρ are functions of the co-moving coordinates (X, Y, Z) determined from the zeroth component of the electromagnetic potential A^μ , i.e.

$$A^\mu = \delta_0^\mu \phi \quad \text{and} \quad U = \frac{1}{1 - \phi}. \quad (2.14)$$

Confining our attention to the spherically symmetric case, the Majumdar–Papapetrou metric can be written as

$$ds^2 = -U^{-2}(R) dt^2 + U^2(R) (dR^2 + R^2 d\Omega^2) \quad (2.15)$$

The metric function U is a function of R only, so (2.13) reduces to

$$\nabla^2 U(R) = R^{-2} (R^2 U'(R))' = -4\pi \rho(R) U^3(R) \quad (2.16)$$

where the prime denotes the differentiation with respect to R . The line element (2.15) can be expressed in the standard form (2.1) through the coordinate transformation

$$r = R U(R) \quad (2.17)$$

with the following relations among the profile functions:

$$B(r) = U^{-2}(R) \quad (2.18)$$

and

$$\frac{1}{\sqrt{A(r)}} = 1 + \frac{R}{U(R)} \frac{dU(R)}{dR}. \quad (2.19)$$

In regions of space where $\rho(R) = 0$ the nonlinear equation (2.16) reduces to a homogeneous equation with the general solution

$$U(R) = k + \frac{m}{R}, \quad (2.20)$$

where k, m , are integration constants. Using (2.17), (2.18), and (2.19), to express the line element in the standard form (2.1) one obtains $B(r) = A(r)^{-1} = k^{-2}(1 - m/r)^2$. If the region of space we are considering extends to $r \rightarrow \infty$, according to the requirements (2.2), we set $k = 1$, and only m remains as a free parameter. The line element is then

$$ds^2 = -\left(1 - \frac{m}{r}\right)^2 dt^2 + \left(1 - \frac{m}{r}\right)^{-2} dr^2 + r^2 d\omega^2 \quad (2.21)$$

which we recognize as the extremal Reissner–Nordstrøm (ERN) spacetime. The general Reissner–Nordstrøm (RN) solution specifies the spacetime metric around a charged point source. Expressing the RN line element in the standard form (2.1) one has $B(r) = A(r)^{-1} = (1 - 2m/r + q^2/r^2)$ where m and q are mass and charge of the source. For $m < q$ the RN spacetime is regular everywhere except at $r = 0$, while for $m > q > 0$, in addition to the singularity at $r = 0$, it exhibits two event horizons located at $r = m \pm (m^2 - q^2)^{1/2}$. In the ERN case, i.e. $m = q$ (gravitational attraction balances electrical repulsion), only one event horizon is present. It is important to note that even if $\rho = 0$ for all R , the solution (2.20) with nonzero m does not specify the metric in the complete spacetime. According to (2.17), the space covered by $0 < R < \infty$ corresponds to the space outside of the shell of the radius $r = m$.

We shall proceed to solve the field equation (2.13) for several choices of electrically counterpoised dust (or extremal charged dust, ECD) distributions $\rho(R)$. Our approach differs from that of Ref. [9] where the solutions to (2.13) are obtained by choosing the function $U(R)$ together with the constraint that the resulting $\rho(R)$ satisfies the non-negativity requirement.

We will consider ECD distributions that effectively vanish at large R so we expect our spacetimes to behave like (2.21) for $R \rightarrow \infty$. The parameter $m_\infty = R(U - 1)|_{R \rightarrow \infty}$, characterizing the asymptotic behavior of $U(R)$ at large R , is the mass seen by the distant observer; we call it the ‘infinity mass’. The behavior of $U(R)$ as $R \rightarrow 0$ can be characterized by the parameter $m_0 = RU|_{R \rightarrow 0}$. The solution is singular at $R = 0$ unless $m_0 = 0$. The singular solutions do not cover the complete spacetime; the metric in the region $0 \leq r \leq m_0$ remains undetermined. If the metric function $U(R)$ is singular at $R = 0$, which corresponds to $r = m_0$, one expects an event horizon at $r = m_0$. Therefore, we may understand the parameter m_0 as the ‘mass below horizon’. If $\rho = 0$ we have $m_0 = m_\infty$, while in case of non-vanishing ECD density ρ we have

$$m_\infty = m_0 + m_\rho \quad (2.22)$$

where m_ρ is the contribution of ECD to the ‘infinity mass’. The ‘ECD mass’ m_ρ is the space integral of the ECD density ρ

$$m_\rho = 4\pi \int_0^\infty \rho U^3 R^2 dR = 4\pi \int_{m_0}^\infty \rho A^{1/2} r^2 dr. \quad (2.23)$$

We conclude this Section by pointing out, for later convenience, that if certain $U(R)$ and $\rho(R)$ solve the equation (2.16), one is allowed to rescale the functions

$$\begin{aligned} U(R) &\longrightarrow U^*(R) = U(\alpha R) \\ \rho(R) &\longrightarrow \rho^*(R) = \alpha^2 \rho(\alpha R) \end{aligned} \quad (2.24)$$

which, as a consequence, rescales the mass parameters according to

$$m \longrightarrow m^* = m/\alpha. \quad (2.25)$$

These relations will help us compare field configurations corresponding to different mass parameters.

III. GENERAL ECD DISTRIBUTIONS AND BIFURCATION

We introduce the ECD distribution by choosing $\rho(R)$ that is well localized in the R -coordinate. As our first example we take $\rho(R)$ of the form

$$\rho(R) = \frac{\eta}{24\pi} R e^{-R} \quad (3.1)$$

where η has the role of an adjustable source strength factor and 24π is a normalization constant that renders $4\pi \int_0^\infty \rho R^2 dR = 1$ for $\eta = 1$.

As (2.16) is a second order differential equation we have to impose two boundary conditions onto a solution. As the first boundary condition we use the requirement that the spacetime is asymptotically flat, i.e. $U|_{R \rightarrow \infty} = 1$, and as the second we chose to fix the parameter $m_0 = R U|_{R \rightarrow 0}$. We obtain the solutions by numerical integration [11] of the differential equation. Starting with the solution of (2.16), for source strength $\eta = 0$, i.e., $m_\infty = m_0$, we slowly increase the value of η . Increasing of η evolves the solution toward $m_\infty > m_0$, but surprisingly one may only increase the value of η up to a critical value η_c . The dependence of m_∞ on η in solutions obtained in this way is shown as the lower part of the solution tracks in Fig. 1. The critical points are labeled (a), (d), (g), and (h), and the corresponding values of η_c and m_∞ are given in Table I.

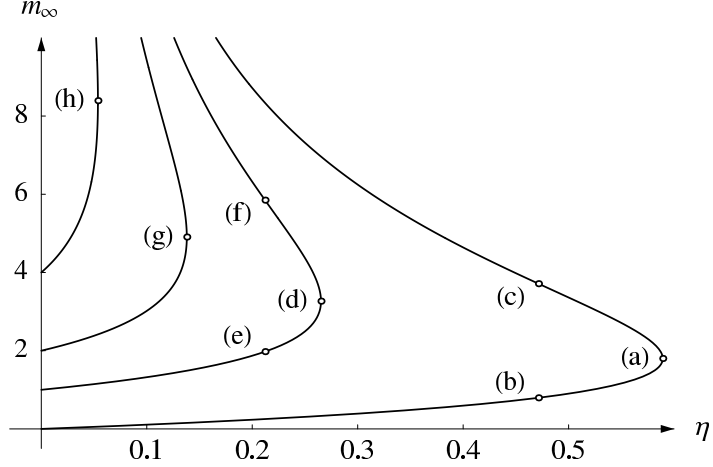


FIG. 1: The dependence of “infinity mass” m_∞ on source strength η in solutions to (2.16) with ECD distribution given by (3.1) and boundary conditions $m_0 = 0$ (leading to regular spacetimes) and $m_0 = 1, 2, 4$ (leading to singular spacetimes). The numerical values of η and m_∞ for the solutions labeled by letters (a–h) are given in Table I.

TABLE I: Numerical values of η and m_∞ for the solutions labeled by letters in Fig. 1

m_0	η_c	$m_\infty(\eta_c)$	$m_\infty^-(\frac{4}{5}\eta_c)$	$m_\infty^+(\frac{4}{5}\eta_c)$
0	0.589272	1.80105 ^(a)	0.795196 ^(b)	3.71325 ^(c)
1	0.265212	3.26661 ^(d)	1.97669 ^(e)	5.84951 ^(f)
2	0.137966	4.90604 ^(g)		
4	0.053701	8.39404 ^(h)		

In addition to these solutions there exists another class of solutions: starting from a critical solution, i.e. one obtained with η_c , in our numerical procedure we could require a slight increase in m_∞ and allow the source strength η to adjust itself freely. The solutions to the differential equation can be found and it turns out that, for this class of solutions, as we increase m_∞ , the source strength η decreases! These solutions are indicated as the upper part of the tracks in the m_∞ vs. η diagram (Fig. 1). Therefore, for source strength $\eta > \eta_c$ there appears to be no solution to (2.16), while if starting from η_c (i.e. from the critical solution such as (a) or (d) in Fig I), the solutions bifurcate by following either lower (through points (b) or (e)) or upper m_∞ -branch (through points (c) or (f)).

In Fig. 1 the critical point on the curve corresponding to the boundary condition $m_0 = 0$

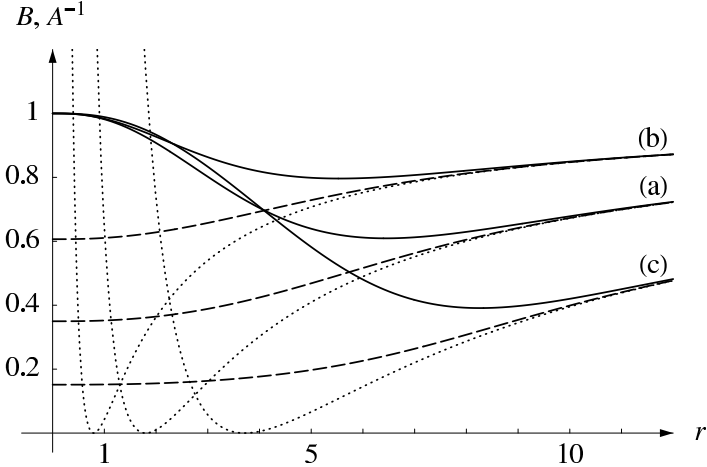


FIG. 2: Regular spacetime metric components $g_{rr}^{-1} = A^{-1}(r)$ (thick lines) and $g_{tt} = B(r)$ (dashed lines) obtained by solving the field equation (2.16) with the ECD distribution given by (3.1) and boundary condition $m_0 = 0$. The solution (a) is the critical solution, while the solutions (b) and (c) are the two independent solutions obtained with $\eta = \frac{4}{5}\eta_c$ (see Fig. 1, and Table I for numerical values). The ERN metric components $A^{-1} = B = (1 - m_\infty/r)^2$ are shown for corresponding m_∞ values (dotted lines).

is obtained with $\eta_c = 0.58927$ and is labeled (a). The points (b) on the lower and (c) on the upper m_∞ -branch indicate the two independent solutions obtained with $\eta = \frac{4}{5}\eta_c = 0.47141$. The corresponding masses are given in Table I. The components of the metric in the r -coordinate $A(r) = g_{rr}$ and $B(r) = g_{tt}$ for the solutions labeled (a), (b), and (c), are shown in Fig. 2. At large r , the metric components $A(r)$ and $B(r)$ coalesce into the ERN metric (2.21). But in contrast to the ERN metric, $A(r)$ and $B(r)$ of our solutions are finite at all r so the spacetime does not involve an event horizon. This is true for all solutions obtained with the boundary condition $m_0 = 0$. We call them the regular solutions, although in Sec. V we show that these solutions may come arbitrarily close to having an event horizon.

The situation is substantially different for the solutions obtained with the boundary condition $m_0 > 0$. The metric components for the case $m_0 = 1$, labeled (d), (e), and (f), in Fig. 1 and Table I, are shown in Fig. 3. At $r = m_0$ the metric component $A(r) = g_{rr}$ diverges ($1/A(r)$ reaches zero) which indicates an event horizon. When approached from $r > m_0$ the functions $1/A(r)$ and $B(r)$ appear to have a double zero at $r = 0$ and in this sense this spacetime singularity is equivalent to the ERN event horizon. Recall that at $r < m_0$ the

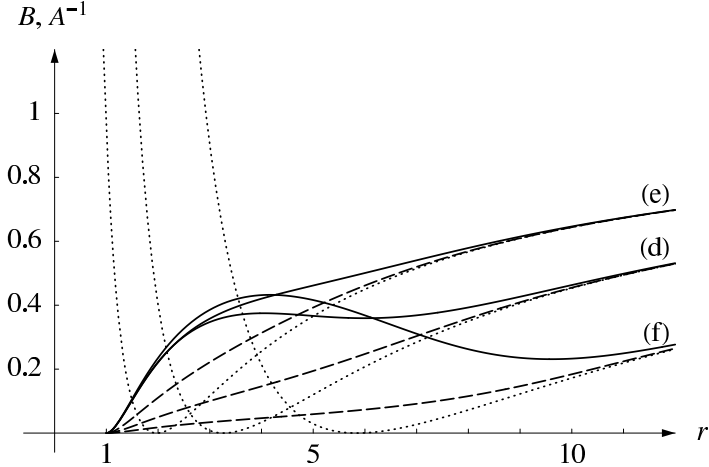


FIG. 3: Regular spacetime metric components $g_{rr}^{-1} = A^{-1}(r)$ (thick lines) and $g_{tt} = B(r)$ (dashed lines) obtained by solving the field equation (2.16) with the ECD distribution given by (3.1) and boundary condition $m_0 = 1$. The solution (d) is the critical solution, while the solutions (e) and (f) are the two independent solutions are obtained for $\eta = \frac{4}{5}\eta_c$, (see Fig. 1, and Table I for numerical values). The ERN profile functions $A^{-1} = B = (1 - m_{\infty}/r)^2$ are shown for corresponding m_{∞} values (dotted lines).

spacetime metric is not specified by the solution to the field equation (2.16). This type of solutions we call singular.

For different choices of ECD distribution ρ , as for instance $\rho(R) \propto R^2 \exp(-R^2)$, basically the same behavior of bifurcating, both regular and singular solutions, occurs. This fact will be used to simplify the treatment of ρ 's in Sec. V.

IV. THE δ -SHELL ECD DISTRIBUTION

Here we will consider the case of ECD distributed on a thin spherical shell of radius R_0 , a situation similar to the one considered by [12]. We set

$$\rho(R) = \eta \delta(R - R_0) . \quad (4.1)$$

Both in the interior ($R < R_0$) and in the exterior ($R > R_0$) space the general solution to (2.16) is of the form (2.20). We set the exterior solution to be asymptotically flat, and we

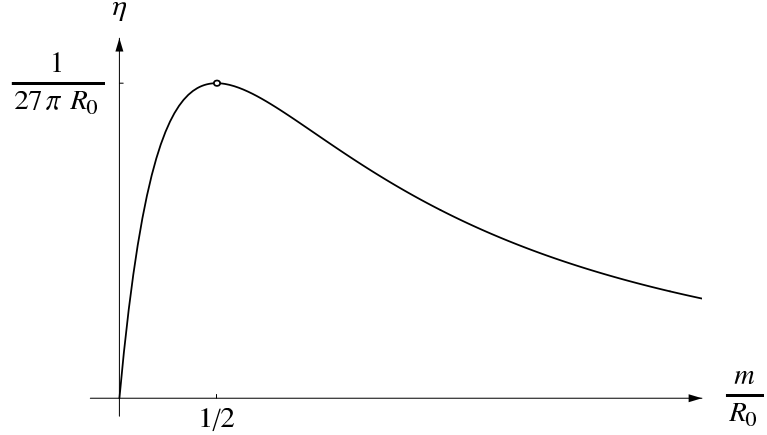


FIG. 4: The source strength η vs. $\xi = m/R_0$ in regular solutions to the field equation (2.16) with δ -shell source (4.1)

allow the interior solution to be singular at $R = 0$:

$$U(R) = \begin{cases} k + m_0/R \equiv U_I & R < R_0 \\ 1 + m_\infty/R \equiv U_E & R > R_0 \end{cases} . \quad (4.2)$$

The requirement that $U_I = U_E$ at $R = R_0$ fixes the value of k

$$k = 1 + (m_\infty - m_0)/R_0 . \quad (4.3)$$

Integration of the differential equation (2.16) with the r.h.s. involving the δ -shell source (4.1) yields

$$R^2 U' \Big|_{R-\epsilon}^{R+\epsilon} = -4\pi R_0^2 \eta U(R_0)^3 . \quad (4.4)$$

When the solution (4.2) is substituted into the above relation the source strength η , m_0 , and the position of the δ -shell source, are interrelated:

$$\eta = \frac{m_\infty - m_0}{4\pi R_0^2} \left(1 + \frac{m_\infty}{R_0} \right)^{-3} . \quad (4.5)$$

This relation leads to bifurcating solutions similar to those discussed in Sec. III.

We now restrict the discussion to the regular solutions, i.e., we set $m_0 = 0$ and proceed with only one mass parameter $m = m_\rho = m_\infty$ given by Eq. (2.23). The source strength (4.5) is

$$\eta = \frac{1}{4\pi R_0} \frac{\xi}{(1 + \xi)^3} \quad (4.6)$$

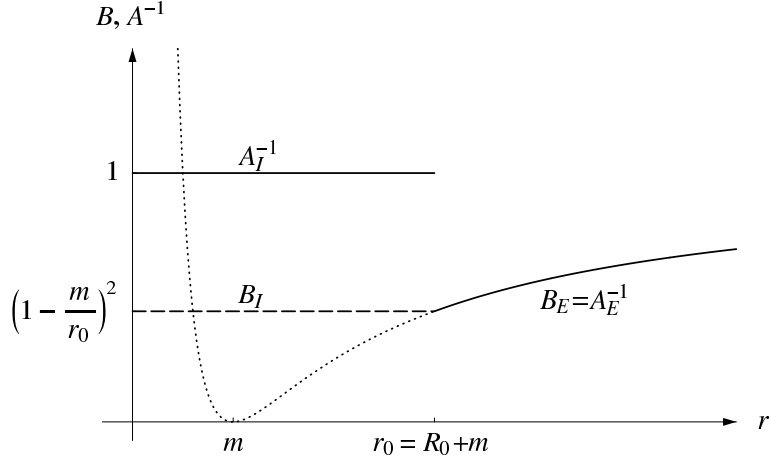


FIG. 5: The metric components $g_{rr}^{-1} = A^{-1}(r)$ (thick line) and $g_{tt} = B(r)$ (dashed line) for the regular critical solution of the field equation (2.16) with δ -shell source (4.1). In the exterior of the shell located at $r_0 = m + R_0$ the metric is equivalent to the ERN (2.21) for the mass m (extended by dotted line into the interior space).

where $\xi = m/R_0$ and it follows that at $\xi_c = 1/2$ there is a maximum $\eta_c = (27\pi R_0)^{-1}$ as shown in Fig. 4. For the regular solution the R -coordinate metric component $U(R)$ is

$$U(R) = \begin{cases} 1 + m/R_0 & R \leq R_0 \\ 1 + m/R & R \geq R_0 \end{cases} \quad (4.7)$$

According to (2.17) the position of the δ -shell in the r -space is $r_0 = m + R_0$. In the interior of the δ -shell the r -space metric components are, according to (2.19) and (2.18), constants

$$A_I^{-1}(r) = 1 \quad \text{and} \quad B_I(r) = \left(1 - \frac{m}{r_0}\right)^2 \quad (4.8)$$

while in the exterior the metric follows the ERN metric given by (2.21). The metric components of only the critical regular solution involving the δ -shell ECD distribution are shown in Fig. 5.

V. UNIFIED TREATMENT OF ECD DISTRIBUTIONS AND QUASI BLACK HOLES

Based on the bifurcation properties of the solutions to the field equation (2.16) discussed in Secs. III and IV we are going to introduce a normalization of the ECD distributions

appropriate for the Majumdar–Papapetrou (MP) formalism. This will allow us to treat the diverse ECD distributions on equal footing and more easily explore their properties. We will focus only on the regular solutions so only one mass parameter $m = m_\rho = m_\infty$ will be used. The ECD distributions considered in Sec. III will be used to generate spacetimes that come arbitrarily close to having event-horizons.

We first consider a general distribution $\rho(R) = \eta \rho_0(R)$ where η is the source strength factor and ρ_0 is normalized so that

$$4\pi \int_0^\infty R^2 \rho_0(R) dR = 1. \quad (5.1)$$

In the linear theory the contribution of $\rho = \eta \rho_0$ to the total mass and charge of the configuration would be $m = q = \eta$, and there would be no upper bound imposed onto the source strength η (see Fig. 6, dotted line). In our case where the field equation (2.16) is non-linear, solutions exist only for values of η less or equal to a critical value η_c . For $\eta = \eta_c$ the solution is unique, we call it the critical solution, and we label the corresponding mass with the symbol m_c . For $\eta < \eta_c$ there are two independent, bifurcating solutions, leading to masses that we label m^\pm where it holds $m_- < m_c < m_+$.

As examples of ECD distributions normalized according to (5.1) we considered

$$\rho_0(R) = n(a, b) R^a \exp(-R^b) \quad (5.2)$$

where a and $b > 0$ are parameters and $n(a, b) = b/(4\pi\Gamma[(3+a)/b])$. The dependence of m on η for the parameter values $a = 0, 1, 2$ and $b = 1, 2$ is shown in Fig. 6. The numerical values for η_c and m_c are given in Table II. As can be seen, only the m^- -branch, and only at the low source strength limit, behaves as it would in the linear theory.

In the context of the field equation (2.16), we can formulate a more natural approach to normalization of the sources by requiring that, for a normalized source $\hat{\rho}$, the critical source strength factor and corresponding mass are both equal to unity, i.e. that $\eta_c = m_c = 1$. Starting from an arbitrarily normalized ECD distribution $\rho_0(R)$ we solve (2.16) to obtain the values η_c and m_c . The normalized source $\hat{\rho}$ is then constructed by rescaling the density ρ_0 according to (2.24) and (2.25) with the scaling parameter $\alpha = m_c$. The MP-normalized source $\hat{\rho}$ corresponding to ρ_0 becomes

$$\hat{\rho}(R) = m_c^2 \eta_c \rho_0(m_c R). \quad (5.3)$$

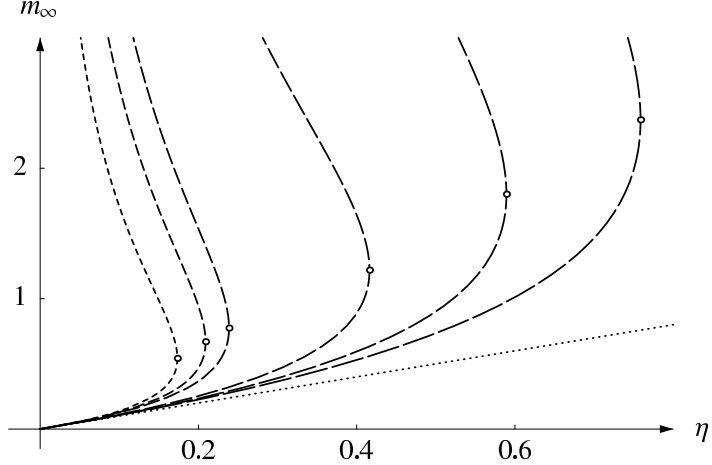


FIG. 6: Dependence of mass m on the source strength η for the regular solutions to the field equation (2.16) with ECD distribution given by (5.2). Going from left to right the tracks are ordered as in the Table II, critical solutions are indicated by circles. Dotted line indicates the expected behavior in the linear theory.

TABLE II: The critical points in the regular solutions to (2.16) obtained with the ECD distribution (5.2)

a	b	$1/n(a, b)$	η_c	m_c
0	2	$\pi^{3/2}$	0.17334	0.542345
1	2	2π	0.209013	0.670181
2	2	$\frac{3}{2}\pi^{3/2}$	0.238647	0.774735
0	1	8π	0.416177	1.21882
1	1	24π	0.589272	1.80105
2	1	96π	0.758753	2.37119

As an example we can take the δ -shell ECD distribution (4.1) discussed in Sec. IV for which we obtained $\eta_c = (27\pi R_0)^{-1}$ and $m_c = R_0/2$ (see Fig. 4). Normalized δ -shell density follows as $\hat{\rho}(R) = (1/54\pi) \delta(R - 2)$. In the case of the ECD distributions (5.2) the MP-normalized version reads

$$\hat{\rho}(R) = m_c^{a+2} \eta_c n(a, b) R^a \exp(-(m_c R)^b) \quad (5.4)$$

where η_c and m_c are obtained numerically (see Table II).

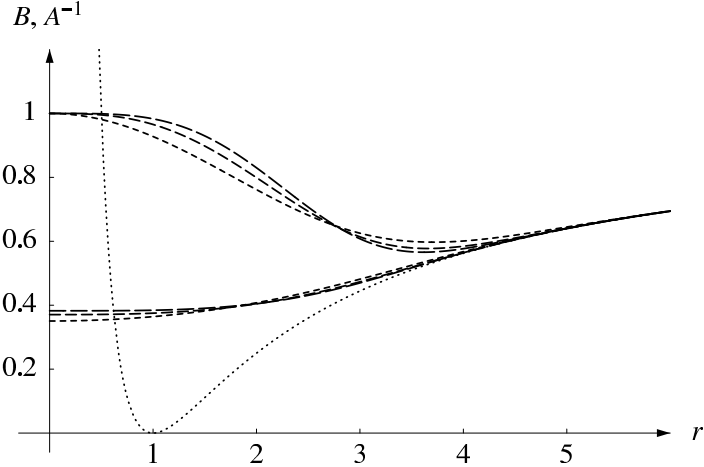


FIG. 7: The r -space metric components $1/A$ and B (dashed) for the critical regular solutions obtained with the first three MP-normalized sources of Fig. 6 and Table II (dashed), and for $m = 1$ ERN metric components (dotted). (Also to be compared with metric components in Fig. 5.)

Using a MP-normalized ECD distribution $\hat{\rho}$, the critical regular solution to the field equation (2.16) is obtained with the source strength $\eta = \eta_c = 1$. The r -coordinate metric components of the critical regular solutions to (2.16) and the ECD distribution (5.4) with parameters $a = 2$ and $b = 0, 1, 2$ are shown in Fig. 7. At large r metric components A and B coalesce into the $m = 1$ ERN metric, while at the intermediate values where major part of the ECD is distributed they are manifestly regular and do not show significant dependence on the choice of the shape of the ECD distribution. By using $\eta < 1$ these solutions can, due to the bifurcating behavior, either evolve toward flat space along m^- branch, or toward higher mass configurations along the m^+ branch. Any of these solutions can be rescaled to describe a unit mass configuration if the rescaling according to (2.24) and (2.25) is carried out with the scaling parameter $\alpha = m$. Starting from the critical solutions shown in Fig. 7 we followed the m^+ -branch to obtain the field configurations corresponding to $m^+ = 10$ and $m^+ = 100$ which we then rescaled to restore the unit mass field configurations. The metric components of these solutions are shown in Fig. 8.

It is plausible that, by following the m^+ -branch toward higher masses and then rescaling the solutions to describe the $m = 1$ configurations, the minimum of the function $1/A(r)$ is deeper and closer to $r = 1$. Asymptotically, in the region $r > 1$ the metric components $A(r)$ and $B(r)$ follow the ERN metric and as the point $r = 1$ is approached from $r > 1$

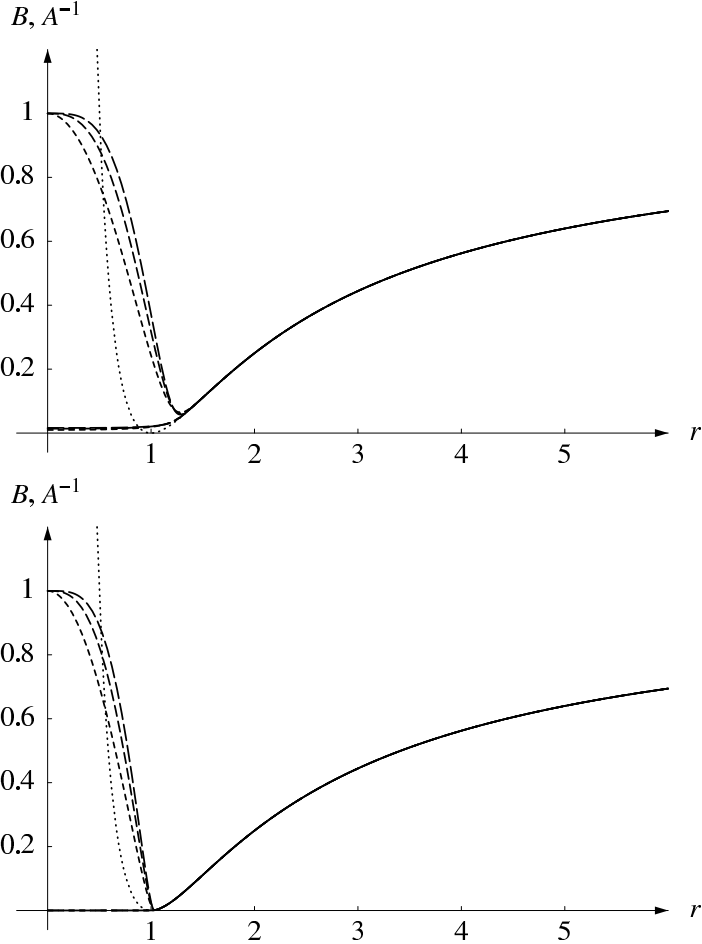


FIG. 8: The r -space metric components obtained by using the MP-normalized sources as in Fig 7 to generate $m^+ = 10$ (upper panel) and $m^+ = 100$ (lower panel) regular solutions which were then rescaled to describe unit mass objects. $m = 1$ ERN metric (dotted)

there appears to be a double zero both in $1/A(r)$ and $B(r)$. In the $r < 1$ region we would asymptotically have $B = 0$ which would not allow for timelike intervals. However, since our spacetimes are everywhere regular, and such a situation is realized only asymptotically, we can consider a radially moving photon for which $ds^2 = 0$ and $d\omega^2 = 0$, so $dt/dr = \pm\sqrt{A/B}$. The ratio of the metric components $\sqrt{A/B}$ for the $m^+ = 10$ /rescaled solutions, related to the time required for the photon to transverse a unit distance in the r -coordinate, is shown in Fig. 9.

The distributions of the ECD for the solutions of Fig. 8 are shown in Fig. 10. Asymptotically, as we would go higher on the m^+ -branch, and rescale to restore unit mass configurations, the density would be completely pulled within the $r = 1$ region. The same was

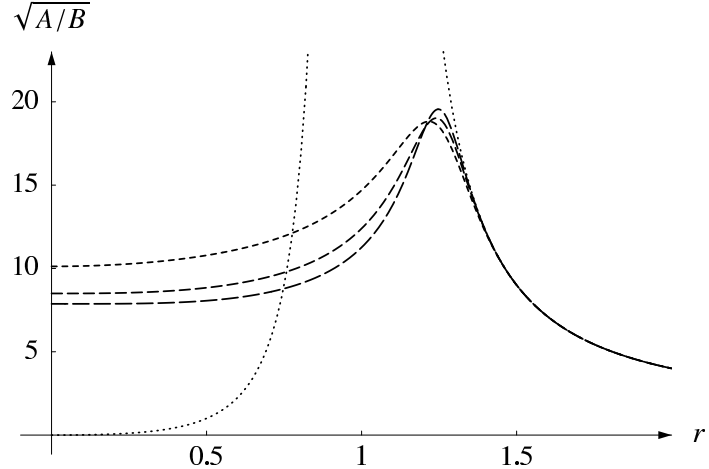


FIG. 9: The ratio $\sqrt{g_{rr}/g_{tt}} = \sqrt{A(r)/B(r)}$ for the solutions shown in Fig. 8 (dashed) and for the ERN metric (dotted)

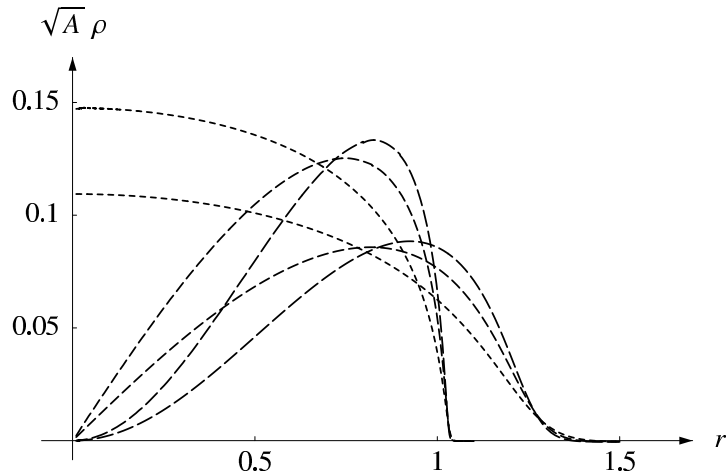


FIG. 10: The density $\sqrt{A}\rho(r)$ for the solutions in Fig. 8. The densities that effectively vanish at $r \simeq 1.1$ correspond to $m^+ = 100$ /rescaled solutions, while those that effectively vanish at $r \simeq 1.5$ correspond to $m^+ = 10$ /rescaled solutions.

obtained by Ref. [9].

VI. CONCLUSIONS

The Majumdar–Papapetrou formalism provides a good environment to study solutions to Einstein–Maxwell equations where matter is assumed to be described by electrically counterpoised dust (ECD). In this paper we have obtained and analyzed regular and quasi black hole

solutions stemming from the M-P formalism and obtained for diverse spherically symmetric ECD distributions by numerical integration of the nonlinear (ordinary differential) field equations. As an immediate consequence of nonlinearity, bifurcating solutions have been identified with respect to an amount of mass allocated in the mass source term. Also an upper bound to the source strength has been found above which no solution exist. Although ECD distributions have assumed analytically different (spherically symmetric) forms, we have been able to reformulate the sources to treat them on equal footing. From this treatment we have been able to obtain regular solutions that come arbitrarily close to black hole solutions. Bifurcation is not an unusual feature in gauge field theory [13] or in gravity [14, 15]. It is encouraging that here we were able to show that the bifurcation described above is not an artifact of a particular choice of charge/matter/energy density. Stability and bifurcation are closely related problems, so investigation of the above solutions with regard to stability is a natural extension of this work.

Acknowledgments

This work is supported by the Croatian Ministry of Science and Technology through the grant ZP 0036038. Authors would like to thank for hospitality the Abdus Salam International Centre for Theoretical Physics, Trieste, Italy, where part of this work was carried out.

- [1] W. B. Bonnor and S. B. P. Wickramasuriya, *Mon. Not. R. Astron. Soc.* **170**, 643 (1975).
- [2] W. B. Bonnor and S. B. P. Wickramasuriya, *Int. J. Theor. Phys.* **5**, 371 (1972).
- [3] W. B. Bonnor, *Class. Quantum Grav.* **15**, 351 (1998).
- [4] J. R. Oppenheimer and H. Snyder, *Phy. Rev.* **56**, 455 (1939).
- [5] S. D. Majumdar, *Phys. Rev.* **72**, 390 (1947).
- [6] A. Papapetrou, *Proc. R. Ir. Acad., Sect. A* **51**, 191 (1947).
- [7] A. Papapetrou, *Z. Phys.* **139**, 518 (1954).
- [8] W. B. Bonnor, *Class. Quantum Grav.* **16**, 4125 (1999).
- [9] J. P. Lemos and E. J. Weinberg, *Phys. Rev. D* **69**, 104004 (2004).

- [10] W. B. Bonnor, Z. Phys. **160**, 59 (1960).
- [11] U. Asher, J. Christiansen, and R. D. Russel, ACM Trans. Math. Softw. **7**, 209 (1981).
- [12] M. Gürses, in *Current Topics in Mathematical Cosmology*, edited by H.-J. Schmidt and M. Rainer (Singapore: World Scientific, 1998), p. 425.
- [13] R. Jackiw and P. Rossi, Phys. Rev. D **21**, 426 (1980).
- [14] Y. Brihaye, F. Grard, and S. Hoorelbeke, Phys. Rev. D **62**, 044013 (2000).
- [15] A. Lue and E. J. Weinberg, Phys. Rev. D **60**, 084025 (1999).